Non-Viral Gene Delivery via Membrane-Penetrating, Mannose-Targeting Supramolecular Self-Assembled Nanocomplexes

Lichen Yin, Ziyuan Song, Kyung Hoon Kim, Nan Zheng, Nathan P. Gabrielson, and Jianjun Cheng*

Gene therapy provides a promising paradigm for the treatment of various acquired or congenital diseases such as cystic fibrosis, severe combined immunodeficiency, diabetes, cancer, and infectious diseases.[1–3] The key challenge in realizing the full potential of gene therapy is the development of efficient yet safe delivery vehicles and methods. Viral vectors, although highly efficient in terms of gene transfection, suffer from immunogenecity, low loading capacity, and challenge of scale-up.[4] As an alternative to viral vectors, non-viral vectors with improved biocompatibility and reduced immunogenicity have been developed. However, clinical application of non-viral vectors has been hampered by their low transfection efficiencies, largely due to the various extracellular and intracellular barriers that act to impede their performance.[5] Hydrolysis of the nucleic acids by ubiquitous nucleases, restricted transfer of non-viral vector/gene complexes across cell membranes, endosomal entrapment, and limited nuclear localization of the genetic cargo all stand as obstacles against effective non-viral gene transfection.[6]

Extensive efforts have been made to improve non-viral gene delivery efficiency through rational and semi-rational design of vectors that are capable of overcoming the various transfection barriers. For instance, cationic lipids and polymers are widely used to condense anionic nucleic acids to improve their stability during transfection and promote cellular internalization.[7–15] Antibodies and targeting ligands are introduced to the vectors to allow receptor-mediated uptake by particular target cells.[16,17] Cell penetrating peptides (CPPs) have been conjugated to or complexed with the nucleic acid cargos to facilitate active cellular internalization and endosomal escape.[18–20] Responsive or degradable polymers have been applied to promote the cytosolic release of the cargo upon internal or external stimuli.[21–28] Nuclear localization signals (NLSs) have been attached to the delivery vector in attempts to aid nuclear delivery.[29] While these strategies have demonstrated success in overcoming individual transfection barriers, the designs are often too complicated or molecule-specific to allow them to be utilized in conjunction with one another. Thus, it is both synthetically and practically challenging to generate a single vector that incorporates all of the rationally designed components in one package to address the aforementioned critical barriers. Although varieties of multifunctional materials, such as the pH-responsive endosomolytic polycation-PEG-DMMAn-Mel nucleic acid carrier developed by the Wagner group[8] and PEGylated glycoproteins developed by the Rice group,[9,30] have been reported to address multiple cellular barriers against non-viral gene delivery, generation of these materials often involve multi-step chemical synthesis and conjugation which may lead to difficulty in quality control and significant batch-to-batch variation. To this end, supramolecular chemistry provides a powerful and convenient approach for the preparation of nanostructured materials from molecular building blocks.[31,32] By relying on the self-assembly and molecular recognition of individual components to formulate nanostructures rather than synthetic chemistry, lead vectors can be easily identified via the combinatorial selection of substrates.[33]

Herein we describe the development of supramolecular self-assembled nanocomplexes (SSANs) by utilizing both rational design and combinatorial selection to identify promising non-viral gene delivery vectors. The SSANs consist of the following rationally designed or selected building blocks: oleyl-conjugated trimethyl chitosan (OTMC), poly(γ-(4-((2-(piperidin-1-yl)ethyl) aminomethyl)benzyl-L-glutamate) (PVBLG-8), oleyl-PEG-mannose (OPM), and plasmid DNA encoding luciferase (pCMV-Luc) (**Figure 1**A). OTMC is a hydrophobic derivative of trimethyl chitosan (TMC), the latter of which was developed previously as an effective candidate for gene delivery with desired biocompatibility and biodegradability profiles.[34,35] Because hydrophobic domains facilitate interactions with cellular/endosomal membranes, OTMC is expected to display better transfection efficiencies by aiding promoted cellular internalization and endosomal escape.[36] OTMC was synthesized by trimethylation of chitosan (200 kDa) and subsequent conjugation of amine-reactive oleyl-NHS to the resultant TMC. The degrees of quarternization and oleyl conjugation were determined to be 25.1% and 16.9%, respectively, as calculated from ^{1}H NMR spectra (Supporting Information, Figure S1). PVBLG-8 is a cationic α-helical polypeptide we recently developed which exhibits potent membrane penetration capacities related to its helical structure.[37,38] PVBLG-8 adopts a stable α-helical structure in aqueous solutions of pH 1–9 (Supporting Information, Figure S2), thereby allowing the polypeptide to maintain its

Dr. L. Yin, Z. Song, K. H. Kim, N. Zheng, Prof. J. Cheng
Department of Materials Science and Engineering
University of Illinois at Urbana-Champaign
1304 W Green St, Urbana, IL 61801, USA
E-mail: jianjunc@illinois.edu
Dr. N. P. Gabrielson
Institute of Genomic Biology
University of Illinois at Urbana-Champaign
1206 W Gregory Drive, Urbana, IL 61801, USA
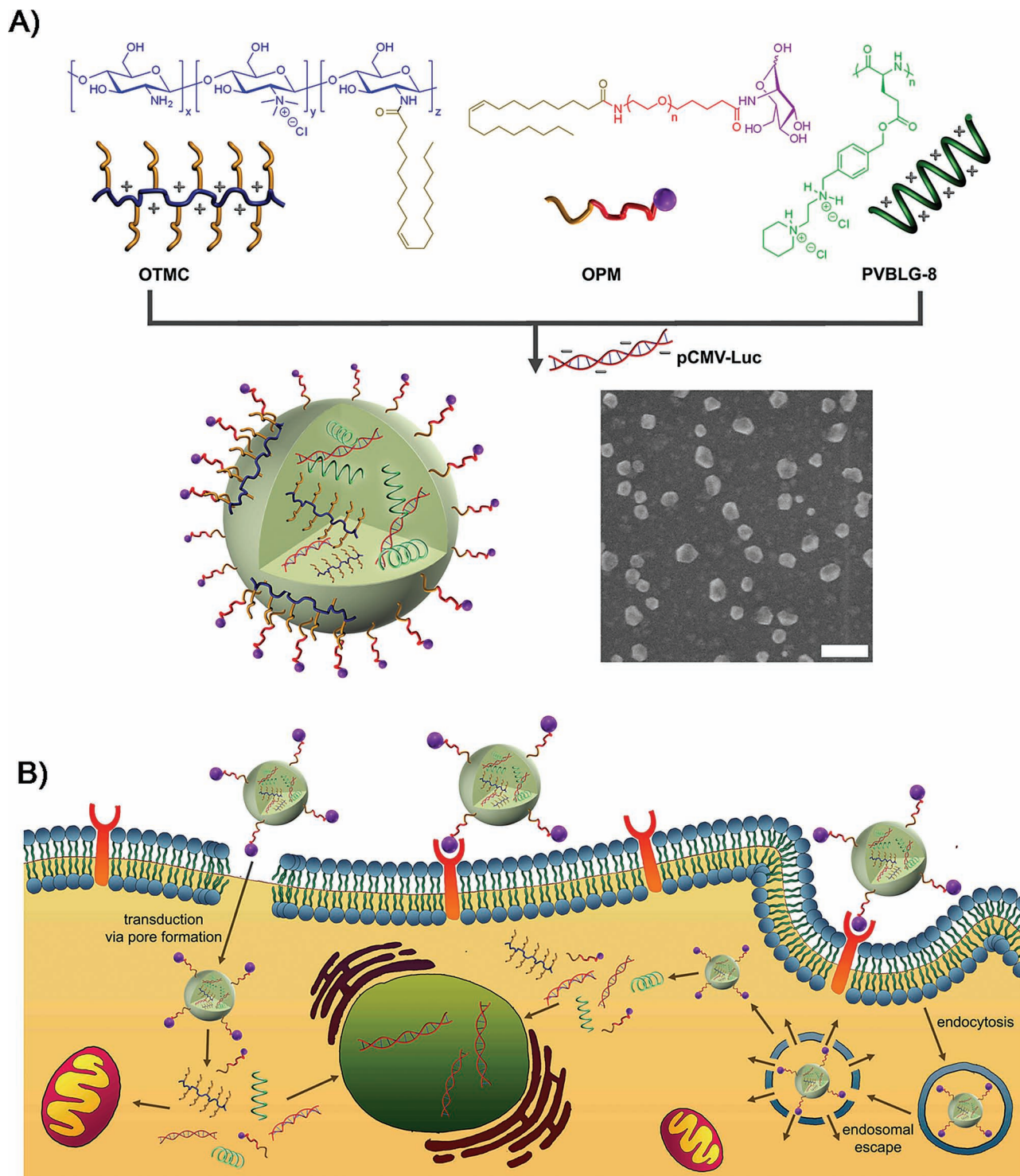
Figure 1. Schematic illustration showing the formation of SSANs and their intracellular kinetics. A) Construction of SSANs via electrostatic as well as hydrophobic interactions among individual components, and SEM image of the resulting SSANs. The scale bar represents 200 nm. B) Schematic representation showing that SSANs targeted to cell membranes via OPM-mediated mannose-receptor recognition entered the cells via endocytosis, as well as direct diffusion via PVBLG-8-mediated pore formation, escaped from endosomes via PVBLG-8-triggered membrane destabilization, and ultimately transferred the DNA to the nuclei to allow gene transcription.

helicity-dependent membrane activity at both neutral extracellular pH and acidic endosomal/lysosomal pH. We incorporated PVBLG-8 (degree of polymerization of 195, polydispersity of 1.1) into the SSANs in attempts to facilitate effective gene transfection by promoting cellular internalization as well as endosomal escape of DNA (Figure 1B). A variety of mammalian

cells, exemplified by macrophages and hepato-carcinoma cells, have over-expressed mannose receptors.[39,40] Therefore, OPM is designed to target SSANs to these cell types and promote the intracellular delivery of DNA (Figure 1B). OPM was synthesized via sequential conjugation of D-mannosamine and oleyl-NHS onto Boc-PEG-SVA, and its final composition was verified by MALDI-TOF MS.

SSANs were prepared via a combination of electrostatic and hydrophobic interactions between each molecular building block. OTMC is an amphiphilic molecule and the key building block of SSANs. It co-condenses DNA with PVBLG-8 via electrostatic interaction and interacts with OPM via hydrophobic interactions with their shared oleyl moieties. By varying the relative amounts of individual components in the SSANs, we aimed to identify the particular combinations that allowed each component to work synergistically and to perform its intended role without impairing the remaining components. Complexes were first prepared from OTMC and pCMV-Luc to obtain an estimated range of OTMC/DNA weight ratios that were able to form stable complexes. As shown in Figure S3 in the Supporting Information, OTMC condensed DNA at OTMC/DNA weight ratios equal to or greater than 2.5 and prevented the migration of DNA in a 1% agarose gel. Dynamic light scattering (DLS) measurement showed a decrease in the particle size and an increase in the zeta potential as the OTMC/DNA weight ratio increased (Supporting Information, Figure S4). Both size and zeta potential plateaued at the OTMC/DNA weight ratio of 10, indicating condensation of DNA and formation of stable complexes at that weigh ratio.

At fixed OTMC/DNA weight ratios of 10, 15, and 20, we incorporated PVBLG-8 at PVBLG-8/DNA weight ratios of 5, 10, 15, and 20. Gel retardation assay revealed complete inhibition of DNA migration with the addition of PVBLG-8, as evidenced by the appearance of a faint band in the loading well. Interestingly, complexes formed with OTMC, PVBLG-8 and DNA displayed reduced DNA fluorescence as compared to complexes formed of only OTMC/DNA (Supporting Information, Figure S5A). This suggested that PVBLG-8 further condensed the anionic DNA to exclude the intercalation of ethidium bromide. Such result was confirmed by DLS measurements, which demonstrated slightly decreased particle size and increased zeta potential as the amount of PVBLG-8 was increased (Supporting Information, Figure S5B). Next, at the fixed OTMC/DNA weight ratio of 15 and fixed PVBLG-8/DNA weight ratios of 10, 15, and 20, OPM was incorporated at 2.5, 5, and 10 mol% relative to OTMC. Complexes showed a slight increase in size and decrease in zeta potential (Supporting Information, Figure S5C), which could be attributed to the OPM layer on the

surface of the complexes that partially shielded the cationic charges. SSANs obtained at the OTMC/PVBLG-8/DNA weight ratio of 15/15/1 and 10 mol% OPM to OTMC revealed spherical morphology and 50–100 nm diameter in the SEM image (Figure 1A).

Upon identifying the optimal range of the OTMC/PVBLG-8/DNA/OPM ratio for complex formation, we next evaluated the ability of the SSANs to protect DNA from nucleolytic degradation. SSANs at the OTMC/PVBLG-8/DNA weight ratio of 15/15/1 with 10 mol% OPM were selected as a representative formulation. DNA degradation was monitored via shifts in the OD_{260} value upon incubation with DNase I. As shown in Figure S5D in the Supporting Information, the OD_{260} of naked DNA increased sharply upon DNase I treatment, indicating enzymatic hydrolysis of DNA according to the hyperchromic effect. In contrast, SSANs showed unappreciable elevation in the OD_{260} value, suggesting that they effectively protected DNA from enzymatic degradation.

The candidate formulations described above were examined for their functionality in transfection assays carried out in the mannose receptor-positive cell lines, HepG-2 and Raw 264.7.[39,40] As shown in **Figure 2**A and Figure S6 in the
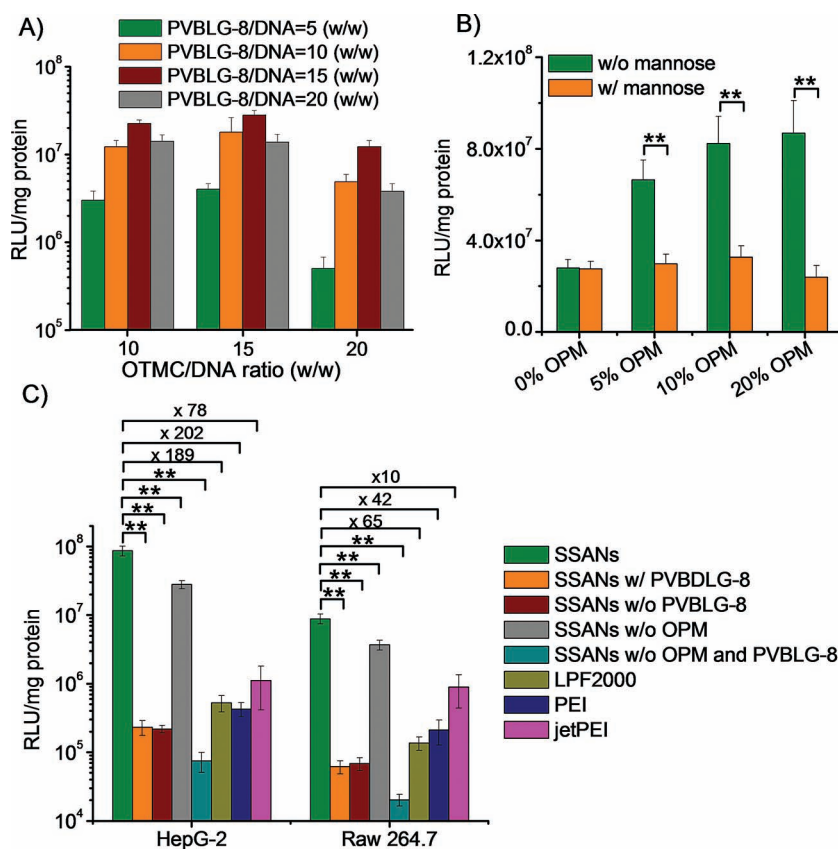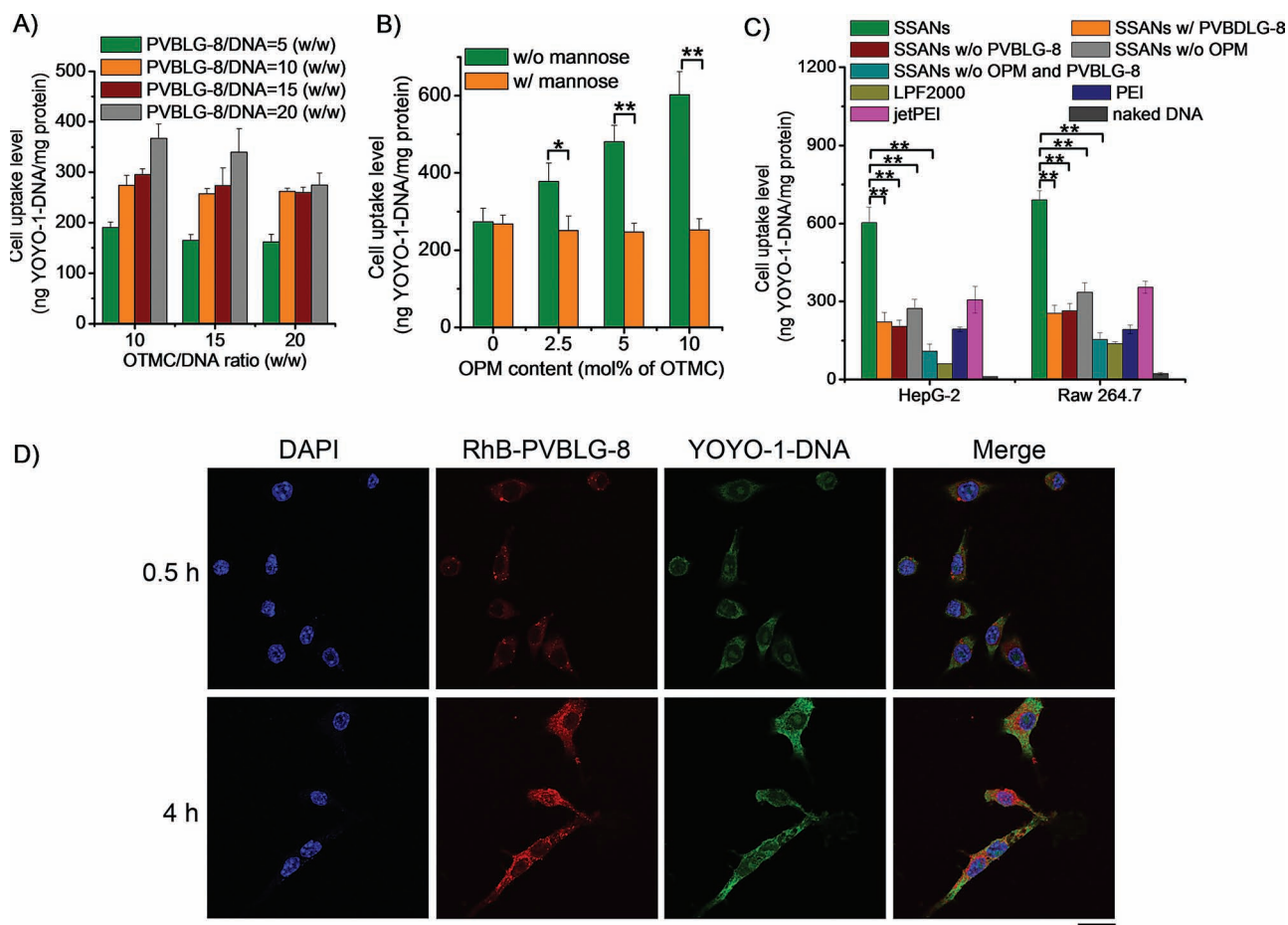

Figure 2. Transfection efficiencies of SSANs in HepG-2 and Raw 264.7 cells. A) Transfection efficiencies of OTMC/PVBLG-8/DNA complexes in HepG-2 cells at various OTMC/DNA or PVBLG-8/DNA weight ratios. B) Transfection efficiencies of SSANs with various OPM contents in HepG-2 cells in the presence or absence of free mannose. The OTMC/DNA and PVBLG-8/DNA weight ratios were kept constant at 15 and 15, respectively. C) A comparative study on the transfection efficiencies of SSANs w/PVBLG-8, w/PVBDLG-8, w/o PVBLG-8, w/o OPM, and w/o PVBLG-8 & OPM. LPF2000, PEI, jetPEI, and naked DNA served as controls. The results were indicated as mean ± standard deviation (SD) ($n = 3$).

Supporting Information, an increase in the OTMC/DNA weight ratio from 10 to 15 and the PVBLG-8/DNA weight ratio from 5 to 15 led to marked elevation in the transfection efficiencies while further increases significantly reduced the transfection efficiency. At the optimal OTMC/PVBLG-8/DNA weight ratio of 15/15/1, OPM was incorporated at 2.5, 5, and 10 mol% relative to OTMC. A 3-4 fold improvement of the transfection efficiency was noted when the OPM content was increased (Figure 2B and Supporting Information, Figure S7), suggesting that SSANs afforded OPM-mediated cell targeting. To further verify the targeting effect, we performed the transfection study in the presence of 600 μmol/L mannose. As shown in Figure 2B and Figure S7 in the Supporting Information, free mannose significantly reduced the transfection efficiencies of the targeted OTMC/PVBLG-8/DNA/OPM complexes but not the OTMC/PVBLG-8/DNA complexes, thereby further substantiating the claim that OPM-containing SSANs were targeted to cell membranes via recognition of mannose receptors that could be competitively occupied by free mannose. The optimal SSAN composition for in vitro gene delivery was thus identified to have the OTMC/PVBLG-8/DNA weight ratio of 15/15/1 and 10 mol% OPM to OTMC which outperformed the commercial transfection reagent Lipofectamine 2000 (LPF2000), PEI, and jetPEI-Macrophage (jetPEI) by 65–189, 42–202, and 10–78 folds, respectively (Figure 2C). When PVBLG-8 was removed from the SSANs or replaced by PVBDLG-8 – a random coiled analogue of PVBLG-8 with minimal cell penetration capabilities[38] – the gene transfection efficiency was notably decreased (Figure 2C). This observation verified the essential role of the helical PVBLG-8 to trigger effective gene transfection by facilitating membrane penetration. When both PVBLG-8 and OPM were removed, SSANs displayed further decreased transfection efficiency (Figure 2C), which confirmed their respective functionality in triggering effective gene transfection. Seriously compromised transfection efficiency in the presence of serum is one of the major set-backs of non-viral gene vectors based on cationic polymers.[41] In this regards, we further evaluated the gene transfection efficiencies of SSANs at various serum concentrations. As illustrated in Figure S8 in the Supporting Information, transfection efficiency of SSANs was not compromised in the presence of 10% serum, and was slightly decreased by 1–2 folds with 20% and 30% serum. Such results suggested stable transfection efficiencies of SSANs towards serum. At high serum concentration (50%), an 8-fold decrease in the transfection efficiency was noted.

Because gene transfection efficiencies of non-viral vectors are closely related to their intracellular kinetics, we next evaluated the cell uptake as well as the intracellular fate of the SSANs. DNA was labeled with YOYO-1 and then used to formulate the SSANs. For OTMC/PVBLG-8/DNA complexes, cell uptake level increased at higher PVBLG-8/DNA ratios, suggesting that PVBLG-8 facilitated cellular internalization of SSANs via membrane destabilization (**Figure 3**A and Supporting Information, Figure S9). In support of this observation, removal of PVBLG-8 from the SSANs or replacement by the membrane-inactive PVBDLG-8 resulted in a dramatically decreased uptake level (Figure 3C). In accordance with the gene transfection efficiency, incorporation of OPM to the SSANs resulted in a 2.2-fold increase in DNA uptake level via

targeting to mannose receptors while addition of free mannose blocked any such improvement by competitively occupying the mannose receptors (Figure 3B and Supporting Information, Figure S10). An increase in the OTMC/DNA ratio did not lead to observable improvement in the uptake level, because DNA had already been completely condensed at the weight ratio of 10 and a further increase to 20 did not exert appreciable effect on the DNA condensation. Additionally, the excessive amount of OTMC might compete with the complexes in interacting with the negatively charged cell membranes and mediating cellular uptake of the complexes, which accounted for the slightly reduced cell uptake level at the PVBLG-8/DNA weight ratio of 20. Thus, in terms of the DNA uptake level, the optimum SSAN formulation was determined to contain OTMC/PVBLG-8/DNA at a weight ratio of 10/20/1 with 10 mol% OPM, outperforming commercial transfection reagents by 2-10 folds (Figure 3C). Confocal laser scanning microscopy (CLSM) images further verified that SSANs containing rhoadmine B (RhB)-labeled PVBLG-8 and YOYO-1-DNA were extensively taken up by Raw 264.7 cells (Figure 3D) and the YOYO-1-DNA trafficked to the nuclei post 4 h incubation. One interesting finding was that the formulation of SSANs resulting in the highest transfection levels (OTMC/PVBLG-8/DNA at a weight ratio of 15/15/1 with 10% OPM) differed from the formulation resulting in the greatest cell uptake level (OTMC/PVBLG-8/DNA at a weight ratio of 10/20/1 with 10% OPM). Such discrepancy indicated that higher DNA uptake level did not necessarily lead to higher gene transfection efficiency. This could be potentially attributed to the cytotoxicity of the added materials as well as increased binding with DNA that restricted intracellular DNA release. Ultimately, it was suggested that a proper balance of DNA condensation vs. intracellular unpackaging and membrane activity vs. cytotoxicity was needed to allow maximal gene transfection efficiency of SSANs.

The intracellular fate of non-viral gene vectors is closely related to their internalization pathway, which ultimately dominates the transfection efficiency. For instance, clathrin-mediated endocytosis (CME) often leads to endosomal entrapment and lysosomal degradation of DNA, thus resulting in minimal gene transfection unless the delivery vector is able to trigger effective endosomal escape.[42] Comparatively, DNA internalized via caveolae, a non-acidic and non-digestive route, avoids endosomal entrapment and thus can be directly transported to the Golgi or endoplasmic reticulum to facilitate nuclear transport.[42] Macropinocytosis is another effective route for transfection as macropinosomes are inherently leaky vesicles, thereby facilitating cytosolic release of DNA and avoiding lysosomal degradation.[42] To probe these different pathways, we performed cell uptake studies under chemical or temperature conditions known to selectively inhibit specific uptake pathways. Low temperature (4 °C) incubation was used to completely block energy-dependent endocytosis.[43] The small molecule drug chlorpromazine was used to inhibit CME by triggering the dissociation of the clathrin lattice. Genistein and methyl-β-cyclodextrin (mβCD) were used to impede caveolae uptake by inhibiting tyrosine kinase and depleting cholesterol, respectively. Dynasore was used to inhibit both CME and caveolae by inhibiting dynamin. Wortmannin was used to prohibit macropinocytotic uptake by inhibiting phosphatidyl inositol-3-phosphate.[42] In

Figure 3. Uptake levels of YOYO-1-DNA containing SSANs in HepG-2 and Raw 264.7 cells. A) Cell uptake level of OTMC/PVBLG-8/DNA complexes in HepG-2 cells at various OTMC/DNA or PVBLG-8/DNA weight ratios. B) Cell uptake level of SSANs with various OPM contents in HepG-2 cells in the presence or absence of free mannose. OTMC/DNA and PVBLG-8/DNA weight ratios were kept constant at 15 and 15, respectively. C) A comparative study on the cell uptake level of SSANs w/PVBLG-8, w/PVBDLG-8, w/o PVBLG-8, w/o OPM, and w/o PVBLG-8 & OPM. LPF2000, PEI, jetPEI, and naked DNA served as controls. D) CLSM images of Raw 264.7 cells after treatment with SSANs containing RhB-PVBLG-8 and YOYO-1-DNA at 37°C for 0.5 and 4 h. Bar represents 20 μm. The results are indicated as mean ± SD (n = 3).

addition to the above conditions, chloroquine and bafilomycin A1 were used to explore the endosomal entrapment and escape mechanism of internalized SSANs. Chloroquine buffers the pH of late endosomes/lysosomes to improve the transfection efficiency of vectors which are unable to escape the lysosomal trafficking pathway. Bafilomycin A1 prevents proton transport into endosomes, which in turn inhibits the protonation of proton sponge vectors inside endosomes and ultimately prevents their endosomal escape.[44]

SSANs with (w/) and without (w/o) PVBLG-8 showed notably different internalization mechanisms and intracellular fate. For SSANs w/o PVBLG-8, the cell uptake level was inhibited by ≈80% at 4 °C, suggesting that most of the complexes were internalized via energy-dependent endocytosis (**Figure** 4A and Supporting Information, Figure S11). In our examination of these energy-dependent processes, chlorpromazine exerted the strongest inhibitory effect on uptake (≈70%) while genistein and mβCD only showed slight inhibitory effect; wortmannin had no appreciable effect at all. Collectively, the data indicated

that, in the absence of PVBLG-8, the complexes entered the cells mainly via CME. As verified by the significantly enhanced transfection efficiency in the presence of chloroquine, we showed that complexes lacking PVBLG-8 suffered from endosomal entrapment and lysosomal degradation post internalization via CME, which finally resulted in their low gene transfection efficiencies (Figure 4B and Supporting Information, Figure S12). The transfection efficiency of SSANs w/o PVGLG-8 was also significantly reduced by Bafilomycin A1 (Figure 4B and Supporting Information, Figure S12), indicating that the complexes could partly escape from late endosomes via the proton sponge mechanism. For SSANs containing PVBLG-8, only a 20–30% reduction in the uptake level was noted at 4 °C. Correspondingly, the endocytic inhibitors displayed only a slight (chlorpromazine, genistein, mβCD, dynasore) or unappreciable (wortmannin) inhibitory effect (Figure 4A and Supporting Information, Figure S11). Such observation implied that the majority of the complexes entered the cells via energy-independent permeation, with only a small fraction being internalized via CME or

ADVANCED
MATERIALS

www.advmat.de

COMMUNICATION

Materials
Views
www.MaterialsViews.com
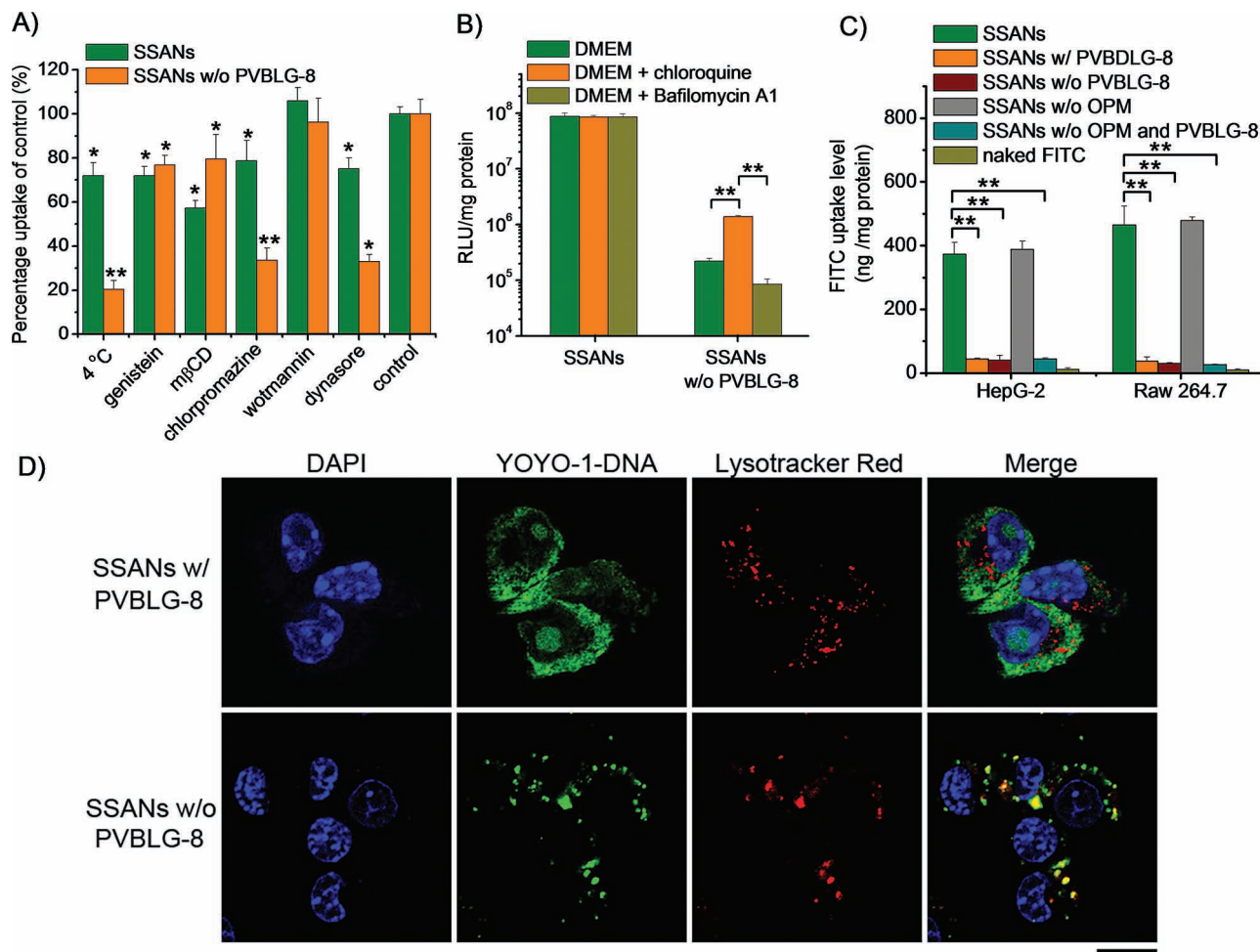
Figure 4. Mechanistic probes of the intracellular kinetics of SSANs. A) Cell uptake level of SSANs in HepG-2 cells in the presence of various endocytic inhibitors. B) Transfection efficiencies of SSANs w/and w/o PVBLG-8 in HepG-2 cells in the presence and absence of chloroquine or Bafilomycin A1. C) Uptake level of FITC in HepG-2 and Raw 264.7 cells following co-incubation with SSANs w/PVBLG-8, w/PVBDLG-8, w/o PVBLG-8, w/o OPM, and w/o PVBLG-8 & OPM for 4 h. D) CLSM images of Raw 264.7 cells treated with SSANs containing YOYO-1-DNA for 4 h and stained with Lysotracker Red. The scale bar represents 20 μm. The results are indicated as mean ± SD ($n = 3$).

caveolae. Chloroquine and Bafilomycin A1 showed unappreciable effects on the transfection efficiency (Figure 4B and Supporting Information, Figure S12), suggesting that SSANs containing PVBLG-8 did not experience late endosomes and escaped from early endosomes by destabilizing endosomal membranes rather than by the proton sponge effect. These results stand as direct evidence that PVBLG-8, with its desired ability to destabilize the cellular as well as endosomal membranes, altered the intracellular kinetics of the SSANs and as a result markedly potentiated the gene transfection efficiency. OTMC/DNA complexes (15:1, w/w), containing neither PVBLG-8 nor OPM, showed similar endosomal escape mechanisms to the SSANs w/o PVBLG-8 (Supporting Information, Figure S13), suggesting that incorporation of OPM had unappreciable effect on the intracellular mechanisms of complexes. CLSM observation was further performed to demonstrate the endosomal escape mechanism of SSANs. As shown in Figure 4D and Supporting Information, Figure S14, punctuated spots of green fluorescence

were observed in the cytoplasm following 4 h incubation with OTMC/DNA complexes or SSANs w/o PVBLG-8, which corresponded to the endocytic vesicles.[45] The green fluorescence (YOYO-1-DNA) largely overlapped with Lysotracker Red-stained endosomes, indicating that the complexes were mainly endocytosed and subsequently entrapped by endosomes. A small proportion of the complexes did not co-localize with endosomes, indicating that OTMC could trigger partial escape from endosome/lysosomes. In the case of SSANs w/PVBLG-8, green fluorescence was extensively spread to the cytoplasm and did not co-localize well with Lysotracker Red, suggesting that PVBLG-8 in the SSANs played important roles in effectively bypassing the endosomes. The green fluorescence was permeated in the cytoplasm, presumably due to the pore formation on cell membranes induced by helical PVBLG-8.[38] To verify such hypothesis, we further explored the cellular uptake level of fluorecein isothiocyanate (FITC), a hydrophilic and membrane-impermeable dye,[45] in the presence of SSANs. As shown in Figure 4C,
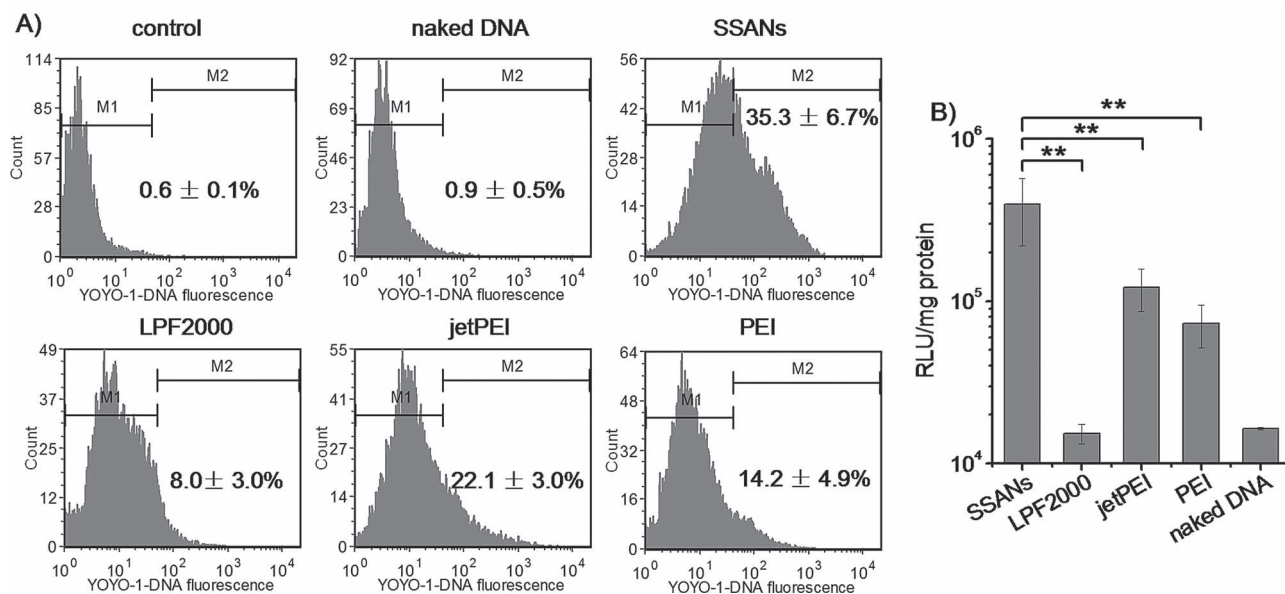
Figure 5. In vivo transfection of SSANs in mouse PECs following i.p. injection at 5 µg pCMV-Luc/mouse. A) Uptake level of SSANs containing YOYO-1-DNA in PECs as monitored by flow cytometry 4 h post administration. M1 and M2 phases corresponded to negative and positive cells, respectively. B) Transfection efficiencies of SSANs in PECs. PECs were harvested 4 h after i.p. injection of SSANs and were further cultured on 96-well plates for 20 h before luminescence measurement. LPF2000, PEI, jetPEI, and naked DNA served as controls. The results are indicated as mean ± SD (n = 4).

FITC was negligibly taken up by cells, which substantiated its impermeability across cell membranes. SSANs led to a 30–50-fold increase in the FITC uptake level, suggesting their capacity to induce pore formation on cell membranes. When PVBLG-8 was removed or replaced by PVBDLG-8, the FITC uptake level was markedly reduced, indicating that the helical PVBLG-8 played essential roles in triggering membrane pore formation. In contrast, when OPM was removed, SSANs displayed negligibly decreased pore-forming capacity.

The cytotoxicity of SSANs was evaluated by assessing the cell tolerability of each individual component and the optimized SSANs (OTMC/PVBLG-8/DNA weight ratio of 15/15/1, 10 mol% OPM) by the 3-(4,5-Dimethyl-2-thiazolyl)-2,5-diphenyl-2H-tetrazolium bromide (MTT) assay. As shown in Figure S15 in the Supporting Information, OTMC and PVBLG-8 showed cytotoxicity towards Raw 264.7 cells at the highest concentration tested (100 µg/mL) while they exerted unappreciable toxicity towards HepG-2 cells at all test concentrations. At the concentrations used for transfection, exemplified by the top-performing SSANs that equaled to the OTMC, PVBLG-8, and OPM concentrations of 15, 15, and 22.5 µg/mL, respectively, none of the materials displayed any significant toxicity. The optimized SSANs also demonstrated minimal cytotoxicity at DNA concentrations lower than 2.5 µg/mL (Supporting Information, Figure S16), further indicating that SSANs were safe while effective non-viral gene vectors.

To test the applicability of SSANs for in vivo gene delivery, we further evaluated the transfection efficiencies of SSANs in murine peritoneal exudate cells (PECs) following i.p. administration and compared with commercial transfection reagents, including LPF2000, PEI, and jetPEI. Flow cytometry analysis showed that ≈35% of the PECs internalized YOYO-1-DNA-containing SSANs 4 h post i.p. injection, which was 1.5–4 fold higher than commercial reagents (**Figure 5**A). SSANs also mediated effective luciferase expression in PECs upon i.p. injection at 5 µg DNA/mouse, significantly outperforming tested commercial reagents (Figure 5B). These results collectively suggested the potential of SSANs in transfecting macrophages in vivo.

In conclusion, we have demonstrated a convenient and modular supramolecular library approach for the preparation of a unique non-viral gene delivery vector that outperformed commercial transfection reagents such as LPF2000, PEI, and jetPEI by 1–2 orders of magnitude in representative macrophages and hepato-carcinoma cells in vitro and by 1.5–4 fold in murine PECs in vivo. Unlike traditional approaches to generate multifunctional materials via multistep chemical synthesis, the rationally selected components were held together via a combination of electrostatic and hydrophobic interactions and worked synergistically to effectively address the various barriers against non-viral gene delivery. Specifically, OTMC condensed anionic DNA into nanoscale complexes, OPM allowed active targeting to cell membranes, and PVBLG-8 facilitated cellular internalization as well as endosomal escape via membrane penetration/destabilization. By modulating the balance between DNA binding strength, membrane penetration capacity, and targeting efficiency, SSANs with maximized gene transfection efficiency and minimized cytotoxicity were identified. We believe that the SSANs described here provide an important addition to existing efforts in identifying cell-specific non-viral gene delivery vehicles. By changing the assembly building blocks in conjunction with the use of a miniaturized high-throughput screening platform, the system could be further optimized and more precisely controlled.

www.MaterialsViews.com

Experimental Section

Experimental materials and methods as well as additional results can be found in the Supporting Information. The animal experimental protocols were approved by the Institutional Animal Care and Use Committees, University of Illinois at Urbana-Champaign, and followed federal and state laws.

Supporting Information

Supporting Information is available from the Wiley Online Library or from the author.

Acknowledgements

[1] M. Candolfi, W. D. Xiong, K. Yagiz, C. Y. Liu, A. K. M. G. Muhammad, M. Puntel, D. Foulad, A. Zadmehr, G. E. Ahlzadeh, K. M. Kroeger, M. Tesarfreund, S. Lee, W. Debinski, D. Sareen, C. N. Svendsend, R. Rodriguez, P. R. Lowenstein, M. G. Castro, Proc. Natl. Acad. Sci. USA 2010, 107, 20021.

[2] F. Yang, S. W. Cho, S. M. Son, S. R. Bogatyrev, D. Singh, J. J. Green, Y. Mei, S. Park, S. H. Bhang, B. S. Kim, R. Langer, D. G. Anderson, Proc. Natl. Acad. Sci. USA 2010, 107, 3317.

[3] C. M. Curtin, G. M. Cunniffe, F. G. Lyons, K. Bessho, G. R. Dickson, G. P. Duffy, F. J. O'Brien, Adv. Mater. 2012, 24, 749.

[4] M. Elsabahy, A. Nazarali, M. Foldvari, Curr. Drug Delivery 2011, 8, 235.

[5] D. W. Pack, A. S. Hoffman, S. Pun, P. S. Stayton, Nat. Rev. Drug Discovery 2005, 4, 581.

[6] Y. J. Kwon, Acc. Chem. Res. 2012, 45, 1077.

[7] M. S. Shim, Y. J. Kwon, Biomaterials 2011, 32, 4009.

[8] M. Meyer, A. Philipp, R. Oskuee, C. Schmidt, E. Wagner, J. Am. Chem. Soc. 2008, 130, 3272.

[9] C. P. Chen, J. S. Kim, D. J. Liu, G. R. Rettig, M. A. McAnuff, M. E. Martin, K. G. Rice, Bioconjugate Chem. 2007, 18, 371.

[10] J. Sunshine, J. J. Green, K. P. Mahon, F. Yang, A. A. Eltoukhy, D. N. Nguyen, R. Langer, D. G. Anderson, Adv. Mater. 2009, 21, 4947.

[11] J. B. Zhou, J. Liu, C. J. Cheng, T. R. Patel, C. E. Weller, J. M. Piepmeier, Z. Z. Jiang, W. M. Saltzman, Nat. Mater. 2012, 11, 82.

[12] B. R. McNaughton, J. J. Cronican, D. B. Thompson, D. R. Liu, Proc. Natl. Acad. Sci. USA 2009, 106, 6111.

[13] R. Maeda-Mamiya, E. Noiri, H. Isobe, W. Nakanishi, K. Okamoto, K. Doi, T. Sugaya, T. Izumi, T. Homma, E. Nakamura, Proc. Natl. Acad. Sci. USA 2010, 107, 5339.

[14] Y. M. Liu, L. Wenning, M. Lynch, T. M. Reineke, J. Am. Chem. Soc. 2004, 126, 7422.

[15] S. Srinivasachari, K. M. Fichter, T. M. Reineke, J. Am. Chem. Soc. 2008, 130, 4618.

[16] G. Zhang, B. S. Guo, H. Wu, T. Tang, B. T. Zhang, L. Z. Zheng, Y. X. He, Z. J. Yang, X. H. Pan, H. Chow, K. To, Y. P. Li, D. H. Li, X. L. Wang, Y. X. Wang, K. Lee, Z. B. Hou, N. Dong, G. Li, K. Leung, L. Hung, F. C. He, L. Q. Zhang, L. Qin, Nat. Med. 2012, 18, 307.

[17] H. Yu, R. D. Koilkonda, T.-H. Chou, V. Porciatti, S. S. Ozdemir, V. Chiodo, S. L. Boye, S. E. Boye, W. W. Hauswirth, A. S. Lewin, J. Guy, Proc. Natl. Acad. Sci. USA 2012, DOI: 10.1073/pnas.1119577109.

[18] W. Y. Seow, Y. Y. Yang, Adv. Mater. 2009, 21, 86.

[19] E. J. Kwon, S. Liong, S. H. Pun, Mol. Pharmaceut. 2010, 7, 1260.

[20] E. J. Kwon, J. M. Bergen, S. H. Pun, Bioconjugate Chem. 2008, 19, 920.

[21] M. A. Kostiainen, D. K. Smith, O. Ikkala, Angew. Chem. Int. Ed. 2007, 46, 7600.

[22] G. Han, C. C. You, B. J. Kim, R. S. Turingan, N. S. Forbes, C. T. Martin, V. M. Rotello, Angew. Chem. Int. Ed. 2006, 45, 3165.

[23] X. Zhao, L. Yin, J. Ding, C. Tang, S. Gu, C. Yin, Y. Mao, J. Controlled Release 2010, 144, 46.

[24] K. Itaka, T. Ishii, Y. Hasegawa, K. Kataoka, Biomaterials 2010, 31, 3707.

[25] J. A. Cohen, T. T. Beaudette, J. L. Cohen, K. E. Brooders, E. M. Bachelder, J. M. J. Frechet, Adv. Mater. 2010, 22, 3593.

[26] X. A. Jiang, Y. R. Zheng, H. H. Chen, K. W. Leong, T. H. Wang, H. Q. Mao, Adv. Mater. 2010, 22, 2556.

[27] P. S. Xu, S. Y. Li, Q. Li, E. A. Van Kirk, J. Ren, W. J. Murdoch, Z. J. Zhang, M. Radosz, Y. Q. Shen, Angew. Chem. Int. Ed. 2008, 47, 1260.

[28] Y. Lee, K. Miyata, M. Oba, T. Ishii, S. Fukushima, M. Han, H. Koyama, N. Nishiyama, K. Kataoka, Angew. Chem. Int. Ed. 2008, 47, 5163.

[29] Q. L. Hu, J. L. Wang, J. Shen, M. Liu, X. Jin, G. P. Tang, P. K. Chu, Biomaterials 2012, 33, 1135.

[30] Y. Park, K. Y. Kwok, C. Boukarim, K. G. Rice, Bioconjugate Chem. 2002, 13, 232.

[31] H. Wang, S. T. Wang, H. Su, K. J. Chen, A. L. Armijo, W. Y. Lin, Y. J. Wang, J. Sun, K. Kamei, J. Czernin, C. G. Radu, H. R. Tseng, Angew. Chem. Int. Ed. 2009, 48, 4344.

[32] H. Wang, K. Liu, K. J. Chen, Y. J. Lu, S. T. Wang, W. Y. Lin, F. Guo, K. I. Kamei, Y. C. Chen, M. Ohashi, M. W. Wang, M. A. Garcia, X. Z. Zhao, C. K. F. Shen, H. R. Tseng, ACS Nano 2010, 4, 6235.

[33] Y. Liu, H. Wang, K. Kamei, M. Yan, K. J. Chen, Q. H. Yuan, L. Q. Shi, Y. F. Lu, H. R. Tseng, Angew. Chem. Int. Ed. 2011, 50, 3058.

[34] T. Kean, S. Roth, M. Thanou, J. Controlled Release 2005, 103, 643.

[35] O. Germershaus, S. R. Mao, J. Sitterberg, U. Bakowsky, T. Kissel, J. Controlled Release 2008, 125, 145.

[36] A. C. Rowat, N. Kitson, J. L. Thewalt, Int. J. Pharmaceut. 2006, 307, 225.

[37] H. Lu, J. Wang, Y. Bai, J. W. Lang, S. Liu, Y. Lin, J. Cheng, Nat. Commun. 2011, 2, 206.

[38] N. P. Gabrielson, H. Lu, L. C. Yin, D. Li, F. Wang, J. J. Cheng, Angew. Chem. Int. Ed. 2012, 51, 1143.

[39] K. Jain, P. Kesharwani, U. Gupta, N. K. Jain, Biomaterials 2012, 33, 4166.

[40] K. Vonfigura, V. Gieselmann, A. Hasilik, Biochem. J. 1985, 225, 543.

[41] S. Srinivasachari, Y. M. Liu, G. D. Zhang, L. Prevette, T. M. Reineke, J. Am. Chem. Soc. 2006, 128, 8176.

[42] I. A. Khalil, K. Kogure, H. Akita, H. Harashima, Pharmacol. Rev. 2006, 58, 32.

[43] S. E. A. Gratton, P. A. Ropp, P. D. Pohlhaus, J. C. Luft, V. J. Madden, M. E. Napier, J. M. DeSimone, Proc. Natl. Acad. Sci. USA 2008, 105, 11613.

[44] A. Akinc, M. Thomas, A. M. Klibanov, R. Langer, J. Gene Med. 2005, 7, 657.

[45] G. Ter-Avetisyan, G. Tuennemann, D. Nowak, M. Nitschke, A. Herrmann, M. Drab, M. C. Cardoso, J. Biol. Chem. 2009, 284, 3370.